PAPER

Kinetic advantages of microwave activation in the dry reforming of methane: insights gained by SSITKA†

Tatsuya Hamashima,[ab] José Palomo, [iD][b] Manoj Coppens,[b] Hajime Hojo [iD][c] Hisahiro Einaga [iD][c] and Atsushi Urakawa [iD] *[b]

Utilising unexploited methane through its reaction with CO_2 *via* the dry reforming of methane (DRM) has attracted attention. However, there are challenges related to catalyst deactivation and energy consumption due to the highly endothermic nature of the DRM; thus, microwave activation has been proposed to increase energy efficiency by directly heating the catalyst while minimising the heating of the reactor. In this study, we clarify the advantages of microwave heating in terms of more reactive coke formation during the reaction and enhanced reactivity under microwave conditions compared with conventional resistive heating. For the latter, steady-state isotopic transient kinetic analysis (SSITKA) was conducted to gain mechanistic insights, which suggested that microwave heating accelerated CO generation steps. This study shows that microwave activation can be advantageous in terms of reaction kinetics for the DRM.

1 Introduction

The effective utilisation of unexploited methane as chemical feedstock has attracted significant attention. In particular, the dry reforming of methane (DRM), which produces synthesis gas (syngas) by reacting the greenhouse gases methane and carbon dioxide, has been regarded as a promising process for efficiently utilising these molecules found in natural gas and biogas.[1,2] The DRM enables the production of syngas with a ratio that favours the formation of long-chain hydrocarbons and value-added products.[3] Since both molecules are thermodynamically stable, the DRM is a strongly endothermic reaction that requires high temperatures to achieve high yields of syngas, which results in a significant energy requirement.[1] Microwave heating has the potential to save energy. Indeed, microwaves enable the selective and rapid heating of targeted materials or chemical species, which results in high energy efficiency.[4,5] Amini *et al.* reported that

microwave heating can reduce energy consumption by approximately 60–80% compared with conventional heating in various processes such as drying, sintering, and pyrolysis.[5] Moreover, microwave heating has been reported to enhance chemical reaction rates and change product selectivity, which are not observed with conventional heating. Although microwave heating is associated with some potential drawbacks including spark and plasma formation, variation in the electromagnetic properties of materials and temperature measurements as well as difficulty in the scale-up of microwave-based processes, which pose challenges for industrial processes,[5] there is growing interest in the application of microwave heating in various chemical reactions.[6,7] Sharifvaghefi *et al.* investigated the DRM reaction involving conventional and microwave heating using Ni–MgO supported on activated carbon as a catalyst. They reported that methane and carbon dioxide conversions increased under microwave heating, and H_2/CO approached unity.[8]

Despite the potential advantages of the DRM, to the best of our knowledge, there have been no detailed reports on the advantages of microwave heating over conventional heating in the DRM. This is attributed to the uniqueness of microwave heating; unlike conventional heating, microwave heating involves complex factors, such as the catalyst shape and quantity, that can significantly change temperature distribution and heating properties. Additionally, the setup of microwave reactors makes it challenging to perform analysis in the same way as that for conventional heating. Therefore,

[a] Department of Interdisciplinary Engineering Sciences, Interdisciplinary Graduate School of Engineering Sciences, Kyushu University, 6-1, Kasugakoen, Kasuga, Fukuoka 816-8580, Japan

[b] Catalysis Engineering, Department of Chemical Engineering, Delft University of Technology, Van der Maasweg 9, 2629 HZ Delft, The Netherlands. E-mail: A.Urakawa@tudelft.nl

[c] Department of Advanced Materials Science and Engineering, Faculty of Engineering Sciences, Kyushu University, 6-1, Kasugakoen, Kasuga, Fukuoka 816-8580, Japan

in this study, we focus on addressing these challenges using steady-state isotopic transient kinetic analysis (SSITKA) study.

SSITKA is an *in situ* technique to gain information about intrinsic kinetics by analysing surface species and their residence time in relation to the product(s) observed.[9] A major advantage of SSITKA is that it allows the observation of transient response while maintaining the steady-state reaction by selectively perturbing the intermediate and product concentrations using isotopic labeling.[10]

Efstathiou and his group have made significant contributions on the development of SSITKA. Their recent work focused on the CO hydrogenation reaction using SSITKA. They observed the dynamic evolution of the exchange rates of adsorbed CO and active CH_x intermediates by switching between $^{12}CO/H_2$ and $^{13}CO/H_2$ over Co-loaded γ-Al_2O_3 catalysts.[11] They demonstrated that SSITKA allows the investigation of the influence of experimental conditions (temperature, H_2 partial pressure, and CO partial pressure) on the dynamics of CO chemisorption and –CH_x formation and hydrogenation rates. Furthermore, they carried out CO hydrogenation experiments over the 20 wt% Co/MnO_x–Al_2O_3 catalyst combined with SSITKA, which provided valuable information regarding the influence of the Mn/Co molar ratio on the composition and reactivity of active and inactive carbonaceous species.[12] As such, SSITKA is widely employed in the studies of reaction mechanisms under technologically relevant steady-state conditions, playing a crucial role in elucidating reaction pathways by analysing kinetic parameters such as the surface coverage of main intermediates and their turnover frequency. Furthermore, SSITKA does not require a specialised experimental setup around the reactor, allowing reactions to be conducted *via* microwave heating without interference with the setup.

Some studies have reported the DRM reaction mechanisms using SSITKA. For example, Efstathiou and his group also conducted a transient kinetic study, involving SSITKA, on the DRM over $Ni/Ce_{0.38}Zr_{0.62}O_{2-\delta}$,[13] $Ni/Ce_{1-x}Pr_xO_{2-\delta}$,[14] $NiCo/CeO_2$–ZrO_2[15] and $NiCo/Ce_{0.75}Zr_{0.25}O_{2-\delta}$,[16,17] in which they discussed the quantification of carbon-containing intermediates, the relative contributions of CH_4 and CO_2 to carbon deposition, and the role of lattice oxygen in carbon removal. They also studied a Ti-added ceria-based Ni catalyst ($Ni/Ce_{0.8}Ti_{0.2}O_{2-\delta}$) and highlighted that the lattice oxygen in the support adjusted the rate of carbon accumulation.[18] This catalyst showed remarkable carbon resistance during the DRM compared to other ceria-based supported Ni catalysts. They also investigated the influence of the lattice oxygen activation energy on the oxidation of carbon, concluding that higher oxygen mobility enhances CO production and concomitant reduction during carbon accumulation.[19]

Bobin *et al.* studied the DRM using $Ln_x(Ce_{0.5}Zr_{0.5})_{1-x}O_2$ (Ln = Pr, Sm, Pr + Sm; $x = 0.3$) catalysts.[20] They observed that after switching the reactants from $^{12}CH_4 + ^{12}CO_2$ to $^{12}CH_4 + ^{13}CO_2$, no ^{13}C accumulated on the catalyst surface, indicating that carbon-containing intermediates such as carbonates

were negligible. Furthermore, they concluded that the activation of CH_4 and CO_2 occurred *via* independent reaction steps. Additionally, Polo-Garzon *et al.* investigated the average residence time, surface concentration, turnover frequency (TOF), and surface coverage of carbon species during the DRM on a Rh-based lanthanum zirconate pyrochlore catalyst across a wide range of temperatures (400–800 °C) using SSITKA.[21] They observed that the decay of the $^{12}CO_2$ signal was consistently shifted from the inert-reference (Ar) signal, independent of the temperature, indicating that the re-adsorption of $^{12}CO_2$ occurred regardless of the temperature. Furthermore, at moderate and high temperatures, the ^{13}CO signal closely matched the $^{13}CO_2$ signal. This was due to the rapid reoxidation of CO. By contrast, at lower temperatures, the ^{13}CO signal was delayed relative to the $^{13}CO_2$ signal, implying that the reaction rate between CO_2 and CO was lower.

In this study, we elucidated the effects of microwave heating during the DRM by SSITKA. Specifically, we investigated the microwave effect on La–Ni oxide catalysts, which have been extensively studied as non-precious metal catalysts with high tolerance to carbon deposition.[1,20,22–24]

2 Results and discussion

2.1 Catalyst characterization

The XRD pattern of the as-prepared catalyst is shown in Fig. S1a.† The calcined catalyst predominantly consisted of the $LaNiO_3$ perovskite phase, and subsequently, H_2 reduction treatment led to the formation of Ni and La_2O_3 crystal phases under conventional heating and microwave heating (Fig. S1b†). Note that different H_2 temperatures (800 °C (conventional heating) *vs.* 740 °C (microwave heating)) were used for catalyst activation because we aimed to achieve a similar catalyst state after the reduction treatment to compare the reactivity during SSITKA studies. The crystallite sizes of Ni and La_2O_3 were nearly identical under both heating conditions (conventional heating: Ni (44°) = 18 nm, La_2O_3 (46°) = 31 nm; microwave heating: Ni (44°) = 19 nm, La_2O_3 (46°) = 30 nm, all determined by the Scherrer equation). Furthermore, the crystallite size of Ni was considerably larger after H_2 reduction *via* microwave heating at 800 °C (Ni (44°) = 27 nm, La_2O_3 (46°) = 29 nm).

2.2 Catalytic results

Microwave heating, having a localised and material-sensitive nature, has been reported to yield temperature gradients in the catalyst bed.[6,7,25] Therefore, comparisons based on one-point temperature measurements, which are, in general, valid for most laboratory-scale reactors operating under conventional heating conditions, are not enough for microwave heating operations.[26] Therefore, extra information is needed in order to find the most suitable operating temperature that enables a relevant catalytic comparison. To tackle this issue and to set an "equivalent set-point temperature" for microwave-assisted heating conditions and

Industrial Chemistry & Materials

Paper

conventional heating conditions, thermal imaging by infrared thermography was used.

The DRM under conventional heating was first evaluated at 600 °C. The catalytic results, in terms of CH_4 and CO_2 conversions, and infrared thermography images for this experiment are presented in Fig. S2,† where the isothermal operation can be confirmed. For comparison, the catalytic results under microwave heating are shown in Fig. S3† with the corresponding infrared thermography images. When operating at a set-point temperature (based on one-point measurements) of 600 °C, higher CH_4 and CO_2 conversion values were observed under microwave heating. This, as revealed by IR thermography images, was related to temperature gradients in the catalyst bed. In order to find comparable conditions for further SSITKA performed in this study, the set-point temperature of the bed under microwave heating was adjusted until the iso-conversion condition was met for both heating modes. This condition was achieved with a set-point temperature of 540 °C for microwave heating. For both heating methods, the upstream region of the catalyst bed exhibited a lower temperature than the downstream region (Fig. S2 and S3†). While this effect was very small in the case of conventional heating, this gradient was significantly more pronounced under microwave heating. Note that such a thermal gradient is not observed when a microwave-absorbing inactive material, e.g. SiC, is placed in the reactor. The presence of cold spots during the DRM is expected due to the endothermic nature of the reaction,[27] and these differences show that endothermic reactions, such as coke formation and/or CO_2 reduction, are accelerated under microwave heating, as discussed later. It is important to mention that both heating methods resulted in stable activity, enabling the possibility of using SSITKA under these operating conditions.

Fig. S4† shows the CO_2 and CH_4 conversion values obtained during SSITKA under conventional and microwave heating by switching the reactant gas mixture between $^{12}CO_2$ + CH_4 and $^{13}CO_2$ + CH_4. In terms of the set point of the reaction temperature measured using a pyrometer (i.e. one-point IR temperature sensor), a lower set-point temperature condition (490 °C) was used for microwave heating than for conventional heating (600 °C) during SSITKA studies, as previously discussed, to attain the iso-conversion condition. Although the initial activity under conventional heating was relatively high, the conversion gradually decreased and stabilised after approximately 30 min. By contrast, under microwave heating, the catalytic activity reached a steady value from the beginning of the reaction, indicating the differences between the heating method in activating the catalyst and intermediates. CO_2 conversion was similar in both heating methods. By contrast, the CH_4 conversion was slightly higher under microwave heating (Fig. S5†); consequently, H_2/CO was slightly higher (Fig. S6†). Fig. S7† shows the mass spectrometry (MS) signals during SSITKA under conventional heating (Fig. S7a†) and microwave heating (Fig. S7b†). For conventional heating, before the 1st

switch, the signals for hydrogen and carbon monoxide decreased, while the signals for methane and carbon dioxide increased, indicating a decrease in the catalytic activity from the start of the reaction until the first switch, as confirmed by GC. Due to the dynamic changes in the catalyst and/or intermediate during the reaction time before the first switch, this isotopic exchange process was not accounted for in the analysis. Conversely, for subsequent switching processes, the catalytic system was stable, making it possible to use these data for SSITKA. However, under microwave heating, the concentrations of the gaseous species across all the isotope switching steps remained stable from the start of the reaction, and all data could be used for SSITKA. In SSITKA, ^{13}CO and $^{13}CO_2$ were used; therefore, they are hereafter referred to as CO and CO_2, respectively.

Fig. 1 compares the normalised responses of the product (CO) and reactant (CO_2) and how they evolved over the switching steps under (the 3rd and 5th switch) conventional and (the 1st, 3rd, 5th switch) microwave heating. Remarkably, under conventional heating, CO and CO_2 signals exhibited a delay relative to the Ar signal, and the lag is more pronounced over the switches. By contrast, the CO_2 and CO signals also lagged behind the Ar signal under microwave heating, but the differences among the switching steps were very small. The data of the 2nd and 4th switching steps are also included in Fig. S8† for completeness, showing the same tendency.

The CO formation process in the DRM reaction is generally reported to consist of multiple reaction steps: (1) the methane dissociation on Ni, forming hydrogen and carbonaceous species; (2) the decomposition of CO_2, yielding CO and atomic oxygen; and (3) the oxidation of carbonaceous species by atomic oxygen, forming CO.[28,29]

$$CH_4 \rightarrow C^* + 2H_2 \tag{1}$$

$$CO_2 \rightarrow CO + O^* \tag{2}$$

$$C^* + O^* \rightarrow CO \tag{3}$$

Furthermore, on supports with high affinity for CO_2, such as La_2O_3, CO_2 reacts with the support to form carbonates. These carbonates may then react with carbon species to produce CO (4).[30,31]

$$CO_2 + La_2O_3 + C^* \rightarrow La_2O_2CO_3 + C^* \rightarrow 2CO + La_2O_3 \tag{4}$$

Even after the conversion reached the steady state, the CO_2 signal continued to lag behind the Ar tracer signal. This behaviour is attributed to the reversible adsorption of CO_2 on catalyst sites that are not directly involved in the catalytic cycle. By contrast, the CO signal also lagged behind Ar during the switches, reflecting the accumulation of C-containing surface intermediates formed along the reaction pathway from CO_2 to CO. By contrast, under microwave heating, the transient signals did not show significant changes over the
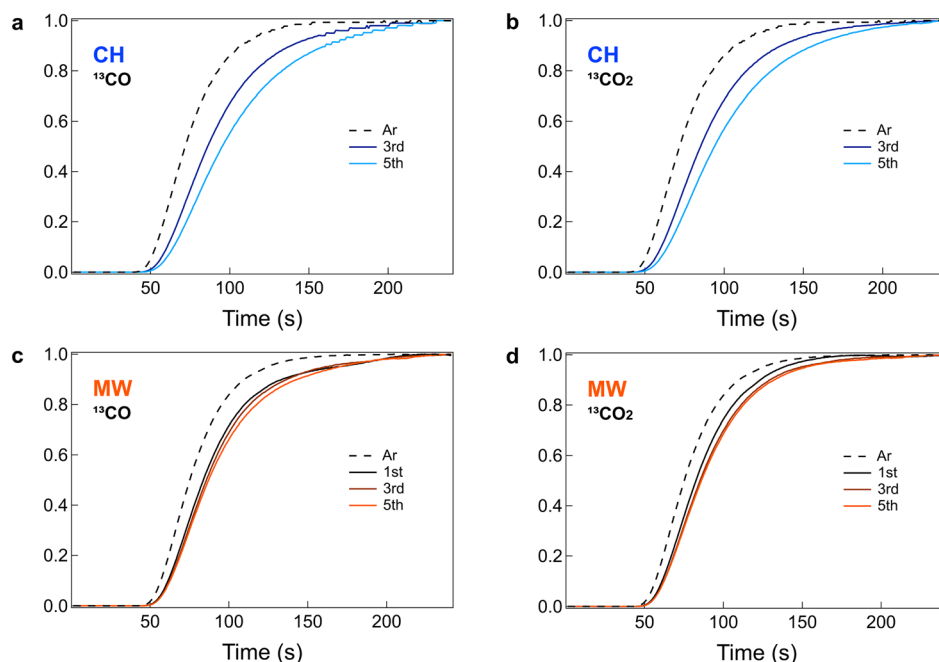
Fig. 1 Normalised and overlaid 3rd and 5th isotope switching steps for the MS signals of (a) CO and (b) CO_2 under conventional heating at 600 °C and 1st, 3rd, and 5th switching steps for the MS signals of (c) CO and (d) CO_2 under microwave heating at 490 °C under the condition of CH_4 : CO_2 = 1 : 1. Owing to the dynamically changing response during the 1st isotopic switch, the reactant (CO_2) and product (CO) responses of the switch are not shown in (a) and (b).

switches, and the delays relative to Ar were smaller than those observed under conventional heating. For CO_2, this may be explained by the suppression of the reversible adsorption of CO_2 during the reaction because CO_2 conversion is comparable between the two heating methods. For CO, the shorter delay is likely attributed to the lower concentration of reactive intermediate species compared to that under conventional heating conditions. The concentrations of CO_2 and intermediate species are estimated in the following section.

To further investigate the influence of carbonaceous species on the catalyst, experiments were performed under the condition where coke formation was favoured with the aim of magnifying the effects related to carbon deposition on the catalyst surface. Carbon deposition is mainly attributed to two reactions, *i.e.*, the methane cracking reaction and carbon monoxide disproportionation reaction. Vasiliades *et al.* quantified the amount of carbon depositions on ceria-supported Ni catalysts and demonstrated that the CO_2 activation route predominates (65.7%) at 550 °C, while the CH_4 decomposition route becomes dominant (54%) at 750 °C, indicating that inactive carbon mainly originates from CO_2 at lower temperatures.[14] In the present study, a CH_4-rich condition was employed to better understand the influence of CH_4-derived intermediates on the catalyst behaviour, surface reactions, and carbon formation under microwave and conventional heating. Additionally, high CO_2 concentrations may lead to catalyst deactivation.[32] Herein, SSITKA experiments were conducted at CH_4 : CO_2 = 2 : 1. As in the previous case, operational conditions (reaction set-point

temperature) were adjusted to have comparable conversion values under conventional and microwave heating conditions.

The steady-state conversion values for CO_2 and CH_4 during the SSITKA experiment are shown in Fig. S9.† Compared to the CH_4 : CO_2 = 1 : 1 condition, it can be seen that the increase in the CH_4-to-CO_2 ratio led to higher CO_2 conversion and an increase in CO formation, regardless of the heating method. This is attributed to the high CH_4 partial pressure, which reduces the surface coverage of oxygen species generated from CO_2 decomposition, thereby increasing the availability of dissociative adsorption sites for CO_2.[30] In particular, under microwave heating, this effect was more pronounced. Furthermore, the ratio of CH_4 conversion to CO_2 conversion was higher under microwave heating, showing a greater difference induced by the heating method compared to the CH_4 : CO_2 = 1 : 1 condition (Fig. S10†). The resulting increased hydrogen production led to a higher H_2/ CO ratio (Fig. S11†). Fig. S12† shows the MS signals obtained during SSITKA under (a) conventional heating and (b) microwave heating. Similar to the previous SSITKA experiments, a relatively higher initial activity was observed at the start of the reaction, followed by a decrease. After the second switching step, the signals stabilised and remained relatively constant. Thus, this first reaction time, including the first isotope switching, was also not accounted for in the analysis. By contrast, under microwave heating, similar to the case of CH_4 : CO_2 = 1 : 1, the responses remained stable and reproducible. Fig. 2 shows the normalised MS signals of CO and CO_2 during the selected switching steps under
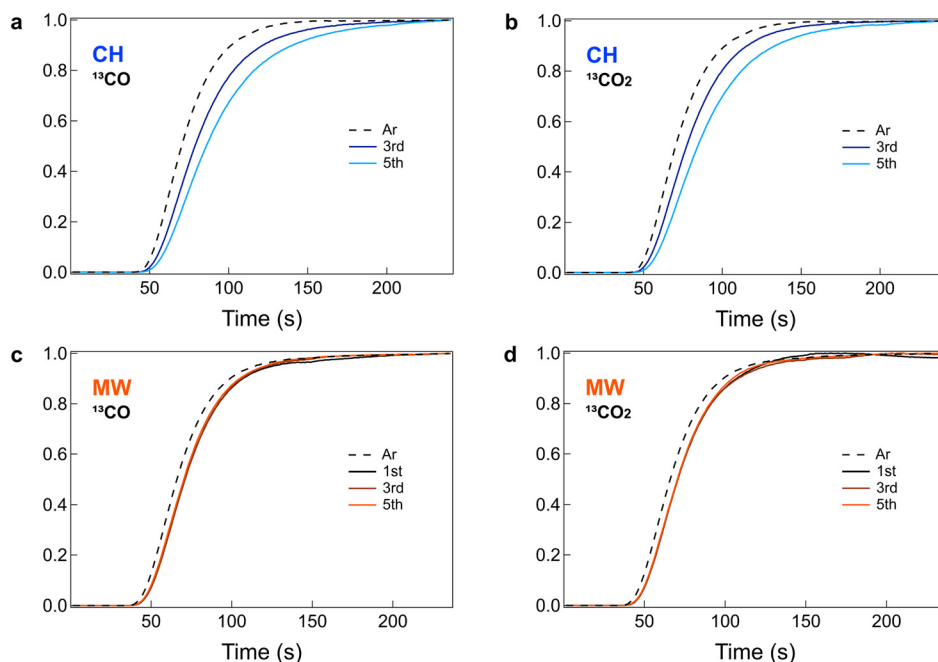
Fig. 2 Normalised and overlaid 3rd and 5th switches for the MS signals of (a) CO and (b) CO_2 under conventional heating at 600 °C and 1st, 3rd, and 5th switches for the MS signals of (c) CO and (d) CO_2 under microwave heating at 490 °C under the condition of $CH_4 : CO_2 = 2 : 1$. Owing to the dynamically changing response during the 1st switch, the reactant (CO_2) and product (CO) responses of the switch are not shown in (a) and (b).

conventional heating and microwave heating. In agreement with previous observations, operations under conventional heating conditions yielded, for CO and CO_2 signals, a prominent delay along each switch. By contrast, under microwave heating, CO_2 and CO exhibited minimal delays relative to Ar, and little variation was observed across different switching steps. These trends were consistently observed in the 2nd and 4th switching steps as well (Fig. S13†). These SSTIKA results qualitatively but evidently show that CO formation is promoted under microwave heating.

In order to discuss the effects of enhanced carbon deposition caused by the high methane partial pressure and the reaction pathways, a quantitative analysis is required. Therefore, in the following section, we estimate the concentration of chemisorbed and intermediate species to enable a more detailed discussion of the reaction mechanisms.

2.3 Estimation of the concentration of chemisorbed CO_2 and intermediate species

Herein, the amounts of carbon-related intermediate species and reversibly chemisorbed CO_2 under steady-state reaction conditions were estimated using eqn (5) and (6), respectively.[14,21]

$$N_C \left(\text{mmol } g_{cat}^{-1} \right) = \frac{y_{CO} F_{total}}{W_{cat}} \int_{t_0}^{t_{ss}} |Z_{Ar}(t) - Z_{CO}(t)| \mathrm{d}t \quad (5)$$
$$= \left| A_{Ar}^{t=t_0-t_{ss}} - A_{CO}^{t=t_0-t_{ss}} \right|$$

$$N_{CO_2} \left(\text{mmol } g_{cat}^{-1} \right) = \frac{y_{CO_2} F_{total}}{W_{cat}} \int_{t_0}^{t_{ss}} |Z_{Ar}(t) - Z_{CO_2}(t)| \mathrm{d}t \quad (6)$$
$$= \left| A_{Ar}^{t=t_0-t_{ss}} - A_{CO_2}^{t=t_0-t_{ss}} \right|$$

Here, y_{CO} and y_{CO_2} represent the molar fractions of CO and CO_2 in the outlet gas stream, respectively. F_{total} represents the total molar flow rate of the feed gas. W_{cat} represents the total amount of the catalyst. $Z_{Ar}(t)$ and $Z_{CO}(t)$ represents the normalised transient responses of each gas. A_{Ar} and A_{CO} represent the calculated areas obtained from the normalised transient MS signals of each gas. t_0 and t_{ss} represent the beginning of the switching step and 200 seconds from the beginning of the increase or decrease in the Ar signal, respectively.

Fig. 3a and b show the amount of reversibly chemisorbed CO_2 under steady-state conditions and the amount of active intermediate species under conventional heating at $CH_4 : CO_2 = 1 : 1$ and $2 : 1$, respectively. Chemisorbed CO_2 exhibited an increase in its amount with each switching step, and it clearly decreased at high methane concentrations, whereas the concentration of the active intermediate remained relatively unchanged. These results suggest that methane-derived intermediates may hinder CO_2 adsorption by acting as barriers on the catalyst surface at high methane concentrations. Fig. 3c and d show the amount of reversibly chemisorbed CO_2 and the concentration of active intermediate species under microwave heating at $CH_4 : CO_2 = 1 : 1$ and $2 : 1$, respectively. Consistent with the trend observed under conventional heating, the concentration of active
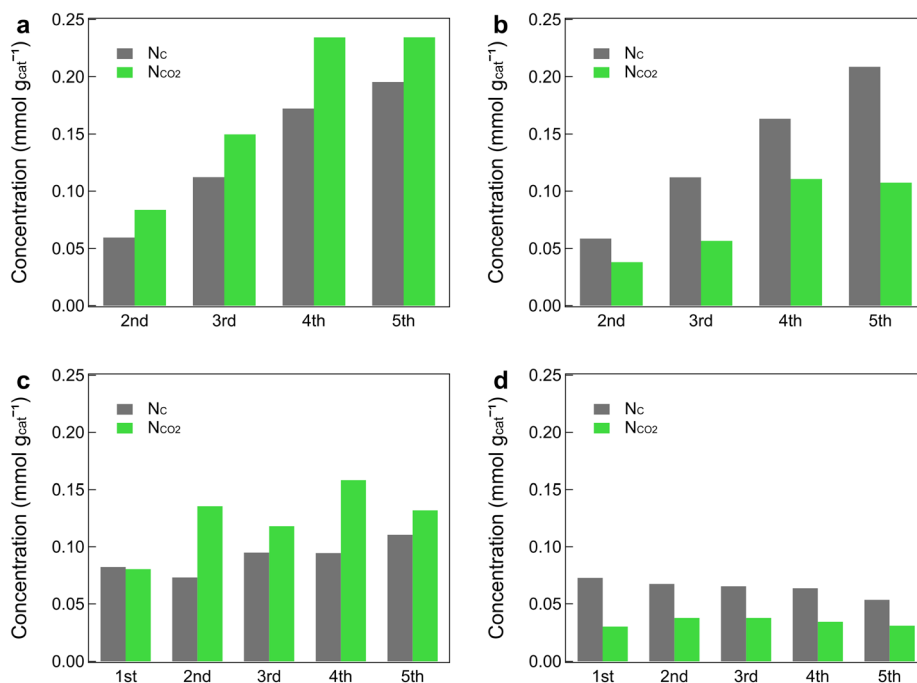
Fig. 3 Estimated concentrations of chemisorbed CO_2 (N_{CO_2}) and active intermediate species (N_C) under conventional heating at (a) $CH_4 : CO_2 = 1 : 1$ and (b) $CH_4 : CO_2 = 2 : 1$ and under microwave heating at (c) $CH_4 : CO_2 = 1 : 1$ and (d) $CH_4 : CO_2 = 2 : 1$.

intermediates clearly decreased at high methane concentrations. However, the increase in the concentration with each switching step was remarkably smaller, and as the reaction progressed, the difference from conventional heating became larger. Although CO_2 conversion was comparable between the different heating methods, the smaller amount of chemisorbed CO_2 suggested that the adsorption–desorption cycle of CO_2 was accelerated under microwave heating. As previously discussed, carbonate species can also be formed during the DRM, along with CO_2 adsorbed on inactive sites. Although the measured catalyst bed temperature was lower under microwave irradiation, the
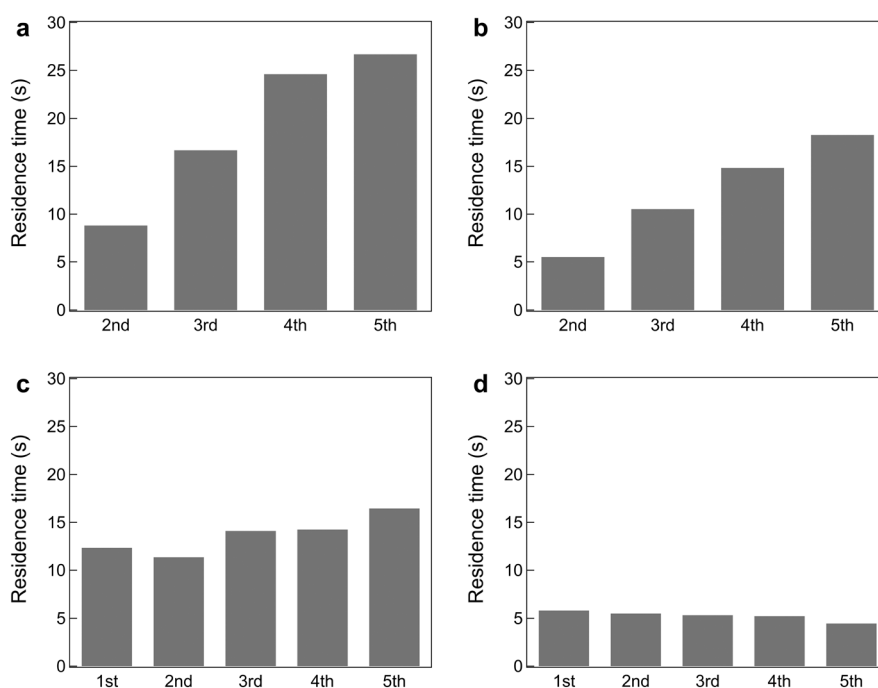

Fig. 4 Estimated CO residence times for the switching steps under conventional heating at (a) $CH_4 : CO_2 = 1 : 1$ and (b) $CH_4 : CO_2 = 2 : 1$ and under microwave heating at (c) $CH_4 : CO_2 = 1 : 1$ and (d) $CH_4 : CO_2 = 2 : 1$.

presence of selectively heated sites, including carbonate species or inactive sites, likely facilitated CO_2 desorption. In parallel, the concentration of active intermediates was also lower under microwave heating. Considering these results, it is possible that oxycarbonate-mediated CO formation on the support contributes to carbon oxidation under microwave heating rather than the direct participation of surface lattice oxygen.

Furthermore, the residence time (τ) of CO was estimated by substituting the normalised MS signal values into eqn (7).[14,21]

$$\tau_{CO}\ (s) = \int_{t_0}^{t_{ss}} |Z_{Ar}(t) - Z_{CO}(t)| dt = |A_{Ar}^{t=t_0-t_{ss}} - A_{CO}^{t=t_0-t_{ss}}| \quad (7)$$

Fig. 4a and b show the residence times under conventional heating at $CH_4:CO_2 = 1:1$ and $CH_4:CO_2 = 2:1$, respectively. As expected from the slower kinetic response of CO (Fig. 1 and 2), the residence time exhibited a gradual increase along each switching step, indicating that the oxidation of methane-derived carbon on the catalyst surface may act as a barrier to the reaction.[28] Fig. 4c and d shows the residence times under microwave heating at $CH_4:CO_2 = 1:1$ and $CH_4:CO_2 = 2:1$, respectively. Compared to conventional heating, the increase in the residence time with each switching step was remarkably smaller, and as the reaction progressed, the difference in the residence time from conventional heating became larger. Especially at $CH_4:CO_2 = 2:1$, the residence time was generally reduced to less than half of the values at $CH_4:CO_2 = 1:1$. This decrease in the residence time at higher CH_4/CO_2 ratios was pronounced under microwave heating conditions (Fig. 4b and d). According to these results, at high methane concentrations, a greater amount of methane-derived carbon is supplied to the catalyst surface, and microwave heating is able to facilitate its oxidation processes.

The differences between the heating methods highlighted above could be related to the carbon species formed during the DRM operation. As previously discussed, microwave heating is material-selective, and carbon materials are well known for exhibiting excellent heating properties under microwave irradiation, allowing them to rapidly and stably reach high temperatures.[33] Owing to this property, carbon-based materials are also utilised as microwave heating susceptors in the DRM.[34] Moreover, heated carbon accumulations, such as coke, may promote CO generation.[35]

Because of the heating properties of the different carbon species formed during the DRM operation, the differences in the heating method can yield differences in the nature of the carbon species formed during the DRM if a specific type of carbon is more reactive under microwave heating. In order to gain insights, we investigated carbon deposits on the spent catalysts. Fig. S14† shows scanning electron microscopy (SEM) images. Carbon filaments (nanotubes) were clearly observed on the spent catalyst after microwave heating, whereas no such carbon filaments were observed after conventional heating. It has been reported that different types of carbon species are deposited during the DRM,

including atomic, polymeric amorphous films, Ni carbides, whiskers, and graphite platelet films, and some of them decrease the activity of the catalyst, while others do not.[36] Therefore, to investigate the reactivity of carbon deposits formed during the DRM operation, temperature-programmed oxidation (TPO) was performed on the spent catalysts, and the results are summarised in Fig. 5. The catalyst tested under conventional heating conditions exhibited a CO_2 evolution peak at around 750 °C, which is mainly attributed carbonate decomposition,[37,38] in addition to some stable carbon deposits that are oxidised at these temperatures. By contrast, the catalyst from the microwave heating operation showed two CO_2 evolution peaks: one centred at a temperature of 750 °C, associated with the decomposition of carbonates and combustion of highly stable carbon deposits, and a second peak at a lower temperature, around 600 °C, corresponding to carbon combustion, presenting a lower stability and higher reactivity.[37,38] It should be noted that there are differences in the set-point temperatures (CH = 600 °C vs. MW = 490 °C), which may influence the nature of the carbon deposits in a localised way. Indeed, various types of carbon species with different reactivities can be generated under DRM conditions,[29,36] which may affect the combustion behaviour during TPO experiments. Although no distinct peaks related to carbon deposits were observed in the Raman spectra (Fig. S15†), TPO results clearly highlight that the coke generated during the microwave heating operation presents a higher reactivity and, thus, is easier to gasify by CO_2 during the DRM operation. The above results indicate that microwave heating exhibits two main features affecting the reaction kinetics of the DRM process, namely, the localised heating of carbon deposits by kinetically accelerating their decomposition by the reaction with CO_2 and the formation of a carbon intermediate species with a higher reactivity, which will also contribute to its faster gasification by CO_2. These two phenomena can explain the differences in the (non-) lagging behaviour observed during SSITKA experiments, with
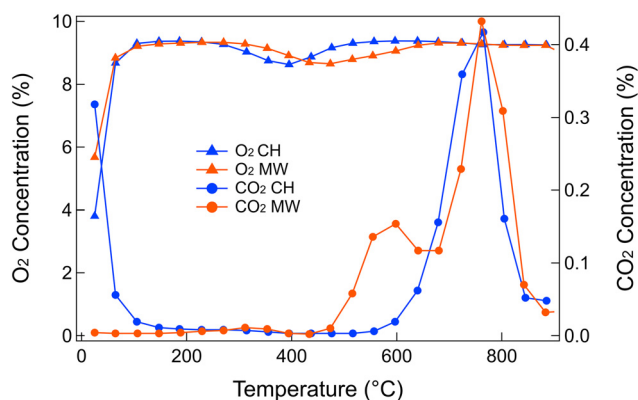

Fig. 5 O_2 and CO_2 concentrations during TPO over the spent catalyst after conventional heating (CH) and microwave heating (MW) at $CH_4:CO_2 = 1:1$. Gas composition = 10% O_2–He balance, flow rate = 50 mL min⁻¹, temperature range = R. T. to 900 °C, and heating rate = 10 °C min⁻¹.

faster kinetics for carbon gasification in the case of microwave heating operations.

3 Conclusions

Understanding the effect of microwave heating on catalytic activity is a critical challenge for improving reaction efficiency, necessitating the development of new analytical techniques to elucidate the underlying mechanisms. In this study, SSITKA was applied to investigate the effects of microwave heating on the DRM by switching the reactant gases between $^{12}CH_4 + {}^{12}CO_2$ and $^{12}CH_4 + {}^{13}CO_2$. The analysis of mass spectrometry signals revealed that under microwave heating, the delay of the CO signal relative to the Ar marker was reduced compared to that under conventional heating. This effect became more pronounced at higher methane concentrations, where the delay relative to Ar was nearly eliminated under microwave heating. A similar trend was observed for the concentration of the intermediate species, which significantly decreased under microwave heating, particularly at high methane concentrations. These findings suggest that microwave heating enhances the oxidation of methane-derived carbon species. TPO results further indicated that highly reactive carbon species accumulated and were subsequently oxidised easily. In summary, the application of SSITKA provided valuable insights into the effects of microwave heating on the DRM. Further studies focusing on more detailed temperature distributions and carbon accumulation will enable a better understanding of the reaction mechanism.

4 Experimental section

4.1 Catalyst preparation

The La–Ni oxide catalyst was synthesised *via* a co-precipitation method. Stoichiometric amounts of La(NO₃)₃·6H₂O (≥99.0%, Fluka Analytical) and Ni(NO₃)₂·6H₂O (≥97.0%, Aldrich) were dissolved in deionised water and then added dropwise using a Pasteur pipette to an aqueous solution of tetramethylammonium hydroxide (TMAH) (35 wt%, Aldrich) under stirring. The mixture was stirred for 30 min and allowed to settle for another 30 min. The resulting precipitate was filtered and dried overnight at 100 °C. The dried precursor was ground using a mortar and pestle for 20 min, followed by calcination at 850 °C for 5 h. The calcined powder was pelletised at a pressure of 4 tons for 1 min and sieved to obtain particles in the 100–300 μm size range.

4.2 Catalyst characterisation

The X-ray diffraction patterns (XRD) of the prepared catalysts were recorded on a Bruker D8 Advance X-ray diffractometer using Cu-Kα radiation (λ = 0.179026 nm) at a scan step of 0.01° s⁻¹ in the region between 5° and 90°. All patterns were background-subtracted to eliminate the contribution of air scattering and possible fluorescence radiation. Scanning electron microscopy (SEM) analyses and energy-dispersive

X-ray spectroscopy (EDS) elemental mappings were carried out using Helios 5 Hydra Dual Beam (Thermo Fisher Scientific).

4.3 Catalytic experiments

Catalytic experiments were carried out under conventional resistive heating (CH) and microwave radiation heating (MW) conditions using a customised laboratory-scale, continuous-flow reaction system with a quartz fixed-bed microreactor (i.d. 4 mm). The schematic of the experimental setup is shown in Fig. S16.† Reactants were introduced using mass flow controllers (MFCs). For resistive heating experiments, the reaction temperature was measured and controlled using a K-type thermocouple inserted at the end of the catalyst bed. For microwave-assisted heating experiments, a Ryowa electronics (MR-2G-100, 2.45 GHz ± 50 MHz, maximum = 100 W) microwave device was used. The temperature of the catalyst was monitored using a one-point IR temperature sensor (TMHXSTMN0050-0070E003, Japan Sensor), and the resonance frequency of microwaves inside the cavity was measured using the detector. With the feedback of these two parameters, the heating power and hence catalyst temperature were controlled. In a typical experiment, 150 mg of LaNiO₃ was mixed uniformly with 50 mg of 80-mesh SiC (98.9%, Cats Import, Hoogvliet) and packed into a quartz reactor. Before starting the reaction, the catalyst was *in situ* reduced by H₂ at 800 °C for 15 minutes in 50% H₂–N₂ gas at 20 mL min⁻¹ using electric (conventional) heating. Upon the completion of the reduction treatment, the catalyst was set to the desired reaction temperature (using the corresponding heating method, MW or CH), and the reaction mixture consisting of 5% CH₄/5% CO₂/50% N₂/40% He at a total flow rate of 50 mL min⁻¹ was introduced. The outlet gas concentration was analysed by gas chromatography (GC; Agilent 7890B, equipped with two FIDs and one TCD) after passing through a water condenser. N₂ was used as the internal standard for GC analyses.

4.4 Visual inspection by digital microscope & IR thermal camera

A digital microscope (×800–1000 magnification) coupled to the reaction system was used for the *operando* monitoring of the catalytic bed. For the visualisation of the temperature in the catalytic bed and the determination of the presence of temperature gradients in the bed, an infrared camera (Micro-SWIR 320CSX Camera, Sensors Unlimited) was also coupled to the reaction system. IR radiation images were converted to temperature distribution images.

4.5 SSITKA (conventional heating)

SSITKA experiments were carried out in a customised laboratory-scale, continuous-flow reaction system provided with a quartz fixed-bed microreactor (i.d. 4 mm) and a gas switching system, which is schematically shown in Fig.

S17.† The flow of all reactants was controlled using mass flow controllers (MFCs). He, Ar, CO_2, and $^{13}CO_2$ were switched between the reactor and the vent line using an automated six-way valve (6WAV1). CH_4 was continuously fed into the reactor by introducing it downstream of the 6WAV1. To avoid any effect related to pressure fluctuations due to gas switching, pressure regulators were installed on the reactor inlet and vent lines, and the pressures at the vent and reactor inlet lines were set to the same value (0.09 bar gauge). The reaction temperature was measured and controlled using a K-type thermocouple inserted at the end of the catalyst bed. In a typical experiment, 150 mg of the catalyst was mixed with 50 mg of SiC and was reduced by H_2 at a high temperature before the reaction. The reduction was performed at 800 °C for 15 min in 50% H_2–He gas at 20 mL min^{-1}. After reduction, the temperature was lowered to 600 °C under a He atmosphere. The composition of the unlabelled reactant gas stream was set to 5% CH_4/5% CO_2/90% He and that of the labelled reactant gas stream was set to 5% CH_4/5% $^{13}CO_2$/85% He/5% Ar. The total flow rate was maintained at 50 mL min^{-1}. Gas switching, between the reactants, was performed every 15 min, with the cycle of $^{12}CH_4 + ^{12}CO_2$ and $^{12}CH_4 + ^{13}CO_2$ repeated three times, resulting in five switches. The concentrations of CO_2 (for $^{12}CO_2$ and $^{13}CO_2$ streams), CH_4, H_2, and CO were analysed using a gas chromatograph (990 Micro GC, Agilent). The transient response of the outlet gases was monitored using a mass spectrometer (HPR-20 EGA, Hidden). To analyse SSITKA results, the MS signals were normalised. For accurate CO signal measurement, the CO fragment was subtracted from CO_2. Additionally, to minimise the influence of noise in steady-state regions, data within 200 seconds from the beginning of the increase or decay of the Ar signal were used. Within this range, the MS signals were normalised by setting the minimum value to 0 and the maximum value to 1.

4.6 SSITKA (microwave heating)

SSITKA experiments were also performed under MW heating conditions. The experimental procedure was the same as that reported in section 4.5, with the following differences. As a heating device, the microwave system, Ryowa electronics microwave apparatus, described in section 4.3, was coupled to the reaction system described in section 4.4. The temperature control was carried out as described in section 4.3. In these SSITKA experiments, the catalyst bed, presenting the same composition as that reported in section 4.5, was *in situ* reduced under microwave heating at 740 °C for 15 min in 100% H_2 gas at 10 mL min^{-1} to avoid over-heating during microwave heating and the formation of microwave-induced plasma by He. Using this reduction treatment, a similar reduction degree to conventional heating was achieved. Then, the catalyst was set to the reaction temperature under a He flow, and the reaction gases were introduced as described above. A preliminary experimental check was conducted to ensure the operation under iso-conversion conditions, with respect to the conventional heating operation.

Data availability

The data supporting this article have been included as part of the ESI.† The authors will upload the figure data in a repository once they are finalised.

Conflicts of interest

The authors declare no conflict of interest.

Acknowledgements

References

1 T. Nguyen, C. L. Luu, H. P. Phan, P. A. Nguyen and T. T. Van Nguyen, Methane dry reforming over nickel-based catalysts: Insight into the support effect and reaction kinetics, *React. Kinet., Mech. Catal.*, 2020, **131**, 707–735.

2 J.-M. Lavoie, Review on dry reforming of methane, a potentially more environmentally-friendly approach to the increasing natural gas exploitation, *Front. Chem.*, 2014, **2**, 81.

3 A. G. S. Hussien and K. Polychronopoulou, A review on the different aspects and challenges of the dry reforming of methane (DRM) reaction, *Nanomaterials*, 2022, **12**, 3400.

4 S. Hamzehlouia, S. A. Jaffer and J. Chaouki, Microwave Heating-Assisted Catalytic Dry Reforming of Methane to Syngas, *Sci. Rep.*, 2018, **8**, 8940.

5 A. Amini, M. Latifi and J. Chaouki, Electrification of materials processing via microwave irradiation: A review of mechanism and applications, *Appl. Therm. Eng.*, 2021, **193**, 117003.

6 X. Zhang and D. O. Hayward, Applications of microwave dielectric heating in environment-related heterogeneous gas-phase catalytic systems, *Inorg. Chim. Acta*, 2006, **359**, 3421–3433.

7 H. M. Nguyen, J. Sunarso, C. Li, G. H. Pham, C. Phan and S. Liu, Microwave-assisted catalytic methane reforming: A review, *Appl. Catal., A*, 2020, **599**, 117620.

8 S. Sharifvaghefi, B. Shirani, M. Eic and Y. Zheng, Application of Microwave in Hydrogen Production from Methane Dry Reforming: Comparison Between the Conventional and Microwave-Assisted Catalytic Reforming on Improving the Energy Efficiency, *Catalysts*, 2019, **9**, 618.

9 A. Holmen, J. Yang and D. Chen, in *Springer Handbook of Advanced Catalyst Characterization*, ed. I. E. Wachs and M. A. Bañares, Springer International Publishing, Cham, 2023, pp. 935–965.

10 A. Urakawa, Methodologies to Hunt Active Sites and Active Species, in *Heterogeneous Catalysts: Advanced Design, Characterization and Applications*, ed. W. Y. Teoh, A. Urakawa, Y. H. Ng and P. Sit, Wiley-VCH, Weinheim, 2021, pp. 363–376.

11 M. A. Vasiliades, N. S. Govender, A. Govender, R. Crous, D. Moodley, T. Botha and A. M. Efstathiou, The effect of H_2 pressure on the carbon path of methanation reaction on co/γ-Al_2O_3: Transient isotopic and operando methodology studies, *ACS Catal.*, 2022, **12**, 15110–15129.

12 M. A. Vasiliades, D. Moodley, R. Crous, J. Potgieter, T. Botha and A. M. Efstathiou, Influence of the Mn promoter on the composition and activity of the adsorbed phase in the carbon paths of the CO hydrogenation reaction on 20 wt % co/MnO_x-Al_2O_3: An operando-SSITKA and transient kinetic study, *ACS Catal.*, 2025, **15**, 5318–5338.

13 M. A. Vasiliades, P. Djinović, L. F. Davlyatova, A. Pintar and A. M. Efstathiou, Origin and reactivity of active and inactive carbon formed during DRM over $Ni/Ce_{0.38}Zr_{0.62}O_{2-\delta}$ studied by transient isotopic techniques, *Catal. Today*, 2018, **299**, 201–211.

14 M. A. Vasiliades, M. M. Makri, P. Djinović, B. Erjavec, A. Pintar and A. M. Efstathiou, Dry reforming of methane over 5wt% $Ni/Ce_{1-x}Pr_xO_{2-\delta}$ catalysts: Performance and characterisation of active and inactive carbon by transient isotopic techniques, *Appl. Catal., B*, 2016, **197**, 168–183.

15 M. A. Vasiliades, P. Djinović, A. Pintar, J. Kovač and A. M. Efstathiou, The effect of CeO_2–ZrO_2 structural differences on the origin and reactivity of carbon formed during methane dry reforming over $NiCo/CeO_2$–ZrO_2 catalysts studied by transient techniques, *Catal. Sci. Technol.*, 2017, **7**, 5422–5434.

16 M. A. Vasiliades, C. M. Damaskinos, P. Djinović, A. Pintar and A. M. Efstathiou, Dry reforming of CH_4 over $NiCo/Ce_{0.75}Zr_{0.25}O_{2-\delta}$: The effect of Co on the site activity and carbon pathways studied by transient techniques, *Catal. Commun.*, 2021, **149**, 106237.

17 M. A. Vasiliades, C. M. Damaskinos, P. Djinović, A. Pintar and A. M. Efstathiou, A transient isotopic study for investigating important design parameters of $NiCo/Ce_{0.75}Zr_{0.25}O_{2-\delta}$ catalyst for the dry reforming of methane, *Catal. Commun.*, 2023, **178**, 106674.

18 C. M. Damaskinos, J. Zavašnik, P. Djinović and A. M. Efstathiou, Dry reforming of methane over $Ni/Ce_{0.8}Ti_{0.2}O_{2-\delta}$: The effect of Ni particle size on the carbon pathways studied by transient and isotopic techniques, *Appl. Catal., B*, 2021, **296**, 120321.

19 M. A. Vasiliades, C. M. Damaskinos, M. Lykaki, S. Stefa, V. D. Binas, T. Kentri, S. Boghosian, M. Konsolakis and A. M. Efstathiou, Deciphering the role of nano-CeO_2 morphology on the dry reforming of methane over Ni/CeO_2 using transient and isotopic techniques, *Appl. Catal., B*, 2024, **350**, 123906.

20 A. S. Bobin, V. A. Sadykov, V. A. Rogov, N. V. Mezentseva, G. M. Alikina, E. M. Sadovskaya, T. S. Glazneva, N. N. Sazonova, M. Y. Smirnova, S. A. Veniaminov, C. Mirodatos, V. Galvita and G. B. Marin, Mechanism of CH_4 Dry Reforming on Nanocrystalline Doped Ceria-Zirconia with Supported Pt, Ru, Ni, and Ni–Ru, *Top. Catal.*, 2013, **56**, 958–968.

21 F. Polo-Garzon, D. Pakhare, J. J. Spivey and D. A. Bruce, Dry Reforming of Mthane on Rh-Doped Pyrochlore Catalysts: A Steady-State Isotopic Tansient Kinetic Study, *ACS Catal.*, 2016, **6**, 3826–3833.

22 N. Bonmassar, M. F. Bekheet, L. Schlicker, A. Gili, A. Gurlo, A. Doran, Y. Gao, M. Heggen, J. Bernardi, B. Klötzer and S. Penner, In Situ-Determined Catalytically Active State of $LaNiO_3$ in Methane Dry Reforming, *ACS Catal.*, 2020, **10**, 1102–1112.

23 Z. Xu and E. D. Park, Recent advances in coke management for dry reforming of methane over Ni-based catalysts, *Catalysts*, 2024, **14**, 176.

24 S. Singh, D. Zubenko and B. A. Rosen, Influence of $LaNiO_3$ shape on its solid-phase crystallization into coke-free reforming catalysts, *ACS Catal.*, 2016, **6**, 4199–4205.

25 T. Durka, T. Van Gerven and A. Stankiewicz, Microwaves in heterogeneous gas-phase catalysis: Experimental and numerical approaches, *Chem. Eng. Technol.*, 2009, **32**, 1301–1312.

26 Y. Wada, S. Fujii and S. Tsubaki, in *Nontraditional Activation Methods in Green and Sustainable Applications*, ed. B. Török and C. Schäfer, Elsevier, 2021, pp. 27–69.

27 D. Pinto, L. Hu and A. Urakawa, Enabling complete conversion of CH_4 and CO_2 in dynamic coke-mediated dry reforming (DC-DRM) on Ni catalysts, *Chem. Eng. J.*, 2023, **474**, 145641.

28 C. Fan, Y.-A. Zhu, M.-L. Yang, Z.-J. Sui, X.-G. Zhou and D. Chen, Density Functional Theory-Asisted Microkinetic Analysis of Methane Dry Reforming on Ni Catalyst, *Ind. Eng. Chem. Res.*, 2015, **54**, 5901–5913.

29 B. Yuan, T. Zhu, Y. Han, X. Zhang, M. Wang and C. Li, Deactivation mechanism and anti-deactivation measures of metal catalyst in the dry reforming of methane: A review, *Atmosphere*, 2023, **14**, 770.

30 V. S. Sandoval-Bohórquez, E. M. Morales-Valencia, C. O. Castillo-Araiza, L. M. Ballesteros-Rueda and V. G. Baldovino-Medrano, Kinetic assessment of the dry reforming of methane over a Ni–la_2O_3 catalyst, *ACS Catal.*, 2021, **11**, 11478–11493.

31 K. Li, F. He, H. Yu, Y. Wang and Z. Wu, Theoretical study on the reaction mechanism of carbon dioxide reforming of methane on La and La_2O_3 modified Ni(1 1 1) surface, *J. Catal.*, 2018, **364**, 248–261.

32 S. de Llobet, J. L. Pinilla, M. J. Lazaro, R. Moliner and I. Suelves, CH_4 and CO_2 partial pressures influence and deactivation study on the Catalytic Decomposition of Biogas over a Ni catalyst, *Fuel*, 2013, **111**, 778–783.

33 T. Kim, J. Lee and K.-H. Lee, Microwave heating of carbon-based solid materials, *Carbon Lett.*, 2014, **15**, 15–24.

34 B. Fidalgo, A. Arenillas and J. A. Menéndez, Mixtures of carbon and Ni/Al_2O_3 as catalysts for the microwave-assisted CO_2 reforming of CH_4, *Fuel Process. Technol.*, 2011, **92**, 1531–1536.

35 J. Hunt, A. Ferrari, A. Lita, M. Crosswhite, B. Ashley and A. E. Stiegman, Microwave-specific enhancement of the carbon–carbon dioxide (boudouard) reaction, *J. Phys. Chem. C*, 2013, **117**, 26871–26880.

36 S. Arora and R. Prasad, An overview on dry reforming of methane: Strategies to reduce carbonaceous deactivation of catalysts, *RSC Adv.*, 2016, **6**, 108668–108688.

37 S. Das, S. Bhattar, L. Liu, Z. Wang, S. Xi, J. J. Spivey and S. Kawi, Effect of Partial Fe Substitution in La$_{0.9}$Sr$_{0.1}$NiO$_3$ Perovskite-Derived Catalysts on the Reaction Mechanism of Methane Dry Reforming, *ACS Catal.*, 2020, **10**, 12466–12486.

38 A. N. Shirsat, M. Ali, K. N. G. Kaimal, S. R. Bharadwaj and D. Das, Thermochemistry of La$_2$O$_2$CO$_3$ decomposition, *Thermochim. Acta*, 2003, **399**, 167–170.